| JMATPRO | Journal of Advanced Materials and Processing<br>9 (3): 3-14, Summer 2021<br>http://jmatpro.iaun.ac.ir<br>20.1001.1.2322388.2021.9.3.1.1 |
|---|---|

Research Paper

# Delamination Detection in a Laminated Carbon Composite Plate Using Lamb Wave by Lead-Free Piezoceramic Transducers

**Mohammad Hossein Ataei[1], Seyed Ali Hassanzadeh-Tabrizi[1*], Mahdi Rafiei[1], Ahmad Monshi[2]**
*1. Advanced Materials Research Center, Department of Materials Engineering, Najafabad Branch, Islamic Azad University, Najafabad, Iran.*
*2. Department of Materials Engineering, Isfahan University of Technology, Isfahan 84156-83111, Iran.*

**ARTICLE INFO**

*Article history:*

Received 8 May 2021
Accepted 6 July 2021
Available online 1 August 2021

*Keywords:*
*Lead-free Piezoceramic*
*Laminated carbon composite*
*Delamination detection*
*Lamb wave*

**ABSTRACT**

The present study develops a semi-instantaneous baseline damage identification approach to identify the delamination damage. An active sensing network with $(Ba_{0.95}Ca_{0.05})(Ti_{0.91}Sn_{0.09})O_3$ (BCTS) lead-free piezoelectric transducers that were mounted on the two undamaged and damaged (with the delamination) plates. The wavelet transform was used for extracting the energy ratio change which is an effective and robust characteristic from the collected time-domain signals. The "identicality coefficient" (IC) was obtained for each sensing path under pristine structural conditions and used to eliminate any inequalities in the signals of each path. The output wave signals of samples were investigated by experiment and the finite element method. The values of the index produced by damages were significant against the threshold value set. The errors were less than 4%, which may be related to the linear relationship considered for the DI and delamination damage. A comparative of sensing paths showed a significant difference between both healthy and damaged samples. The delaminated damage was detected because the delamination phenomenon increased the amplitude of the wave and the wave energy. The comparison of the "damage index" (DI) values of six sensing paths showed that the path with delamination damage had the highest DI value i.e., 0.92 and then the sensing paths closest to the damage showed the highest DI values (DI=0.67). The path with a distance farther from the damage shows DI=0.09. The other DI values of other sensing paths were close to zero (DI=0) due to no damage.

**Citation**: Bakhtiari, L., Jafari, A., Sharafi, Sh., (2021) The Effect of Reverse Pulse Plating and Lanthanum Addition in Plating Bath on Corrosion Resistance of Austenitic Steel in Chlorine Solution, Journal of Advanced Materials and Processing, 9 (3), 3-14. Dor: 20.1001.1.2322388.2021.9.3.1.1



* **Corresponding Author**
E-mail address: hassanzadeh@pmt.iaun.ac.ir

## 1. Introduction

Composite materials have been widely used in many high-performance structures due to their high specific strength and stiffness coupled with cost-effectiveness over traditional materials. Internal damages such as microcracks and delaminations are generated; they can eventually cause catastrophic failures of structures during the service life. Delamination in composite structures plays a major role in lowering structural strength and stiffness, consequently downgrading system integrity and reliability. Therefore, composite structures are needed to be examined frequently. There is an increasing interest in SHM of composite structures as composite materials are widely used in structures. However, composite materials are susceptible to damages such as delamination and debonding. Such defects often occur beneath the surface of the composite structures, and they are hardly visible or detectable by the naked eyes. Further damage may also occur in composite laminates in the form of delaminations between plies of dissimilar properties. Such delaminations are promoted by the interfacial shear and normal stresses that appear in the "boundary layer" at the laminate edges and near internal cracks. Composite materials are vulnerable to damages, including debonding and delamination, due to accumulated fatigue loading or abrupt impact. Delaminations are areas of separation between the layers of a laminate composite or between the faces and the core of a composite sandwich. Disbonds are areas in which two adherends have separated at the bondline. Currently, non-destructive testing (NDT) is performed to detect such damages during inspections, and there are ongoing efforts to develop an online SHM, which can perform automated damage diagnosis during the normal operation. Structural health monitoring is evaluating and assuring the performance and safety of structures using sensor data. In the SHM process, an electric signal applied at the transmitter PWAS generates, through piezoelectric transduction, elastic waves that travel into the structure and are captured at the receiver PWAS. As long as the structural region between the transmitter and receiver is in pristine condition, the received signal will be consistently the same; if the structure becomes damaged, then the received signal will be modified. Comparative of the historically stored signals and the currently read signal will indicate when changes (e.g., damage) take place in the structure. There is an increasing need for a valid, cheap, and fast monitoring system to ensure the functionality and safety of a laminated composite structure. Ultrasonic guided waves, especially Lamb waves, because of their favorable features like low attenuation during propagation, propagating in curved panels, and large-distance traveling in a thin-plate structure, received a lot of attention as an efficient tool for damage identification like delaminations and cracks in composite and metallic structures [1-10]. Because damage identification results based on the Lamb waves propagation approach can be influenced by varying environmental and operational conditions, the development of a robust monitoring system with no need for the prior measured data of the structure has gained much attention recently. Many investigations have utilized the Lamb wave-based damage diagnosis for components with simple geometry like plates to successfully detect debonding and delamination [11-15]. Although ultrasonic guided wave attenuation in carbon-fiber-reinforced polymers is greater than metal alloys, many researchers widely study this method in composite materials [16-21]. Gumez et al. investigated the delamination damage detection in wind turbine blades using guided waves. They developed a new approach for disunity detection between layers comparing two real blades. Also, one of them was built with three disbonds introduced in its manufacturing process. The signals are denoised by Daubechies wavelet transform. The threshold for denoising is obtained by a wavelet coefficients selection rule using the Birgé-Massart penalization method. The signals were normalized, and their envelopes were obtained by Hilbert transform. Finally, pattern recognition based on correlations was applied. Damaged and undamaged blades were compared. The three induced disbonds in the "damaged blade" were clearly found [16]. The signals were normalized, Hilbert transform was used to obtain their envelopes, and pattern recognition was applied based on the correlations. A new technique for damage detection was proposed by Yeum et al. [18]. They detected the delamination in composite plates by comparing pitch-catch Lamb wave signals of a piezoelectric transducer (PZT) network without using their baseline signals from the pristine conditions [18]. It was on the basis of the fact that while the fundamental antisymmetric (A0) mode passes through a delamination area, its speed slows down. On the other hand, delamination slightly affects the fundamental symmetric mode (S0). The $A_0$ modes' relative time delays are instantly compared. Therefore, intense delamination detection is obtained at different temperatures. Kang et al. [22] showed that by using the PZTs, which are embedded in a composite plate, Lamb waves could be generated and used for health monitoring applications. A Lamb wave-based identification method was established to delaminate in vacuum-assisted resin transfer molding (VARTM) composite structures. The finite element method (FEM) experiment was used to propagate Lamb waves in composite plates. The study assessed damage in the plates by fusing information from multiple sensing paths of the embedded network. To eliminate interference, a wavelet transform technique was applied to purify the acquired Lamb wave

signals. The results showed that satisfactory detection of defects could be achieved with the proposed method. Ng et al. [23] for checking the carbon fiber reinforced polymer (CFRP) retrofitted concrete structures debonding, proposed transducers network by sequentially receiving and actuating nonlinear Rayleigh wave. The second harmonic generation nonlinear property was used for debonding due to the Rayleigh wave interaction at the debonding between the concrete interfaces and CFRP. The ultrasonic guided wave propagation technique as a promising method of damage detection utilizes guided waves in the damage detection by the analysis of differences among the signals recorded from sensing paths as baseline data when the structures are in their pristine conditions with no damage. The variations in operational and environmental parameters are a crucial concern with the methods using pristine baseline data, which can make a difference in the structure's currently collected response with that of measured baseline data. Furthermore, the detection of any possible existing initial defect is not possible before installing the sensor. To solve these drawbacks, some techniques have been tried to be developed, which do not require the use of pristine baseline data, such as the time-reversal method. Sohn developed some progress in in-service monitoring of aerospace, automotive, civil, and mechanical systems, which are subject to various operational and environmental. He developed effects of environmental and operational variability on structural health monitoring [24]. A. Marzani, S. Salamo presented a numerical prediction and experimental verification of temperature effect on plate waves generated and received by piezoceramic sensors. This work proposes a numerical approach based on a Semi-Analytical Finite Element (SAFE) model to predict temperature effects on guided waves generated and received by low-profile piezoceramic (PZT) transducers. The proposed model includes the cumulative role of transducer elements (actuator and sensor), substrate structure, and transducer/structure interaction in predicting the full pitch-catch guided wave response under changing temperature. Also, it was presented a novel physics-based temperature compensation model for structural health monitoring using ultrasonic guided waves [25,26]. An analytical and experimental investigation of the Lamb wave-mode tuning with piezoelectric wafer active sensors (PWASs) is presented by G. B. Santoni et al.. The analytical investigation assumes a PWAS transducer bonded to the upper surface of an isotropic flat plate. The PWAS Lamb wave tuning technique described in this paper is used to resolve the side packets problem. Several tuning cases are illustrated [27]. A reference-free scheme was proposed by Kim and Sohn. The proposed NDT technique utilizes the polarization characteristics of the piezoelectric wafers attached on both sides of the thin metal structure. Crack formation creates Lamb wave mode conversion due to a sudden change in the thickness of the structure. Then, the proposed technique instantly detects the appearance of the crack by extracting this mode conversion from the measured Lamb waves, and the threshold value from damage classification is also obtained only from the current dataset [28]. Alem and Abedian proposed a semi-instantaneous baseline approach to detect damage using a guided wave propagation technique with an embedded PZT wafer active sensor [29]. In this method, its introduced IC was obtained and used for all sensing paths in structures' pristine conditions to eliminate any inequalities in the signals of each path. The technique was according to the assumption that the $S_0$ of Lamb waves is attenuated by passing through the crack damage. The damage was detected on a sample lap joint structure by an active sensing network. FEM is used for wave propagation simulation by the wavelet transform to calculate DI values.

The main idea and novelty of the present study is developing a semi instantaneous baseline damage identification to identify the delamination damage in a laminated carbon composite plate. Because damage identification results based on the Lamb waves propagation approach can be influenced by varying environmental and operational conditions, developing a robust monitoring system with no need for the prior measured data of the structure has gained much attention recently. The instantaneous baseline damage detection technique is one of the promising methods that overcome the mentioned obstacles. This method was proposed by Alem and Abedian that used to detect and characterize fatigue cracks that initiate around the rivet holes of lap joint metal structures [29]. The authors developed a semi-baseline damage identification approach for detecting delamination damage for the first time. The obtained results show that this method can detect delamination. The output wave signals, IC, and DI values of each sensing path for healthy and damaged samples were investigated and evaluated by experimental and FEM.

Another novelty and merit of the study is that for the first time, an active sensing network of lead-free BCTS or $(Ba_{1-x}Ca_x)(Ti_{1-y}Sn_y)O_3$ (designed and manufactured by the same authors) was used to damage detection instead of PZT transducers. In order to detect the delamination damage in laminated composite structures by the method of sending and receiving propagated wave with a high piezoelectric sensors coefficient ($d_{33}$), a lead-free piezo ceramic $(Ba_{1-x}Ca_x)(Ti_{1-y}Sn_y)O_3$ with high piezoelectric coefficients ($d_{33}$=752 pC/N) and the corresponding planar electromechanical coupling factor (kp=54.2%)

and inversed piezoelectric coefficient (dS/dE=1248 pm/V) [30]. Also, due to the toxicity of lead, environmental concerns and limitations, there is an immediate demand for lead-free alternatives to PZT transducers and sensors.

## 2. Experimental

### 2.1. Materials and Specimen preparation

Two undamaged and damaged laminated composite plate samples containing four layers prepreg woven carbon/epoxy (Japan Toray 100% quality carbon fiber sheet T300) with plies angles "0/90, ±45, Teflon, ±45, 0/90", shaped at 0.001 in×7.36 in×7.36 in, were prepared as experimental specimens. Fig. 1 shows a schematic of the dimension and geometrical information of the samples. In the delaminated region, a thin Teflon tape was used to separate two delamination surfaces in the delamination region with the individual lamina distance. Also, Fig. 2 shows a laminated carbon composite plate with delamination damage. Table 1 shows the mechanical properties of the specimen. Also, the sensors used in this study were BCTS, whose properties are given in Table 2. These designed and manufactured transducer sensors were used for the first time on a composite plate for damage detection [30]. An arrangement of four BCTS transducer sensors was used for the active sensing network, as illustrated in Fig. 3. In order to bond the sensors to the specimens' surface, a conductive silver epoxy adhesive (CW2400) was utilized.

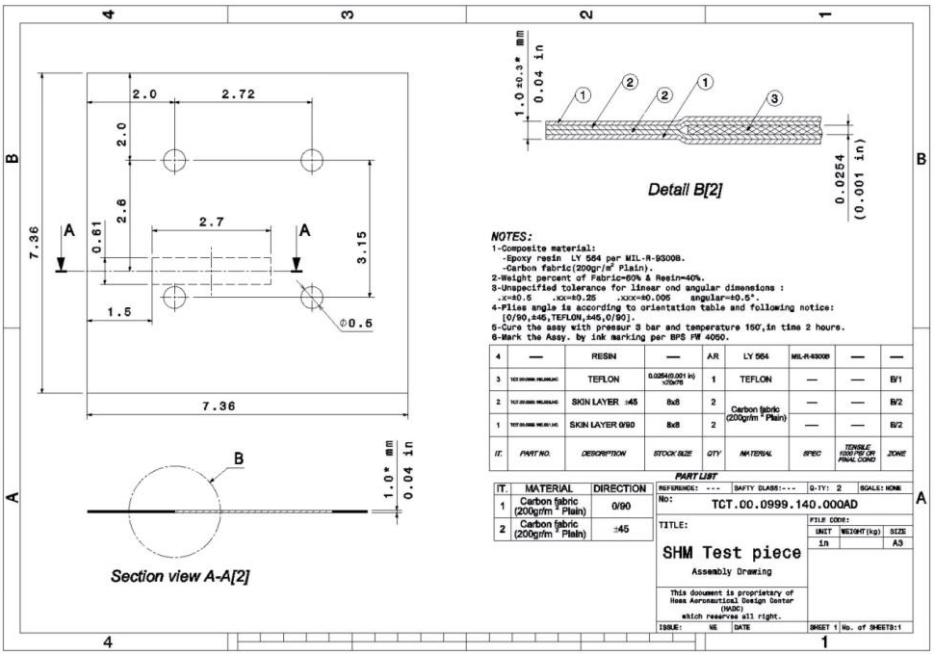


**Fig. 1.** Schematic of dimension and geometrical information of the samples.

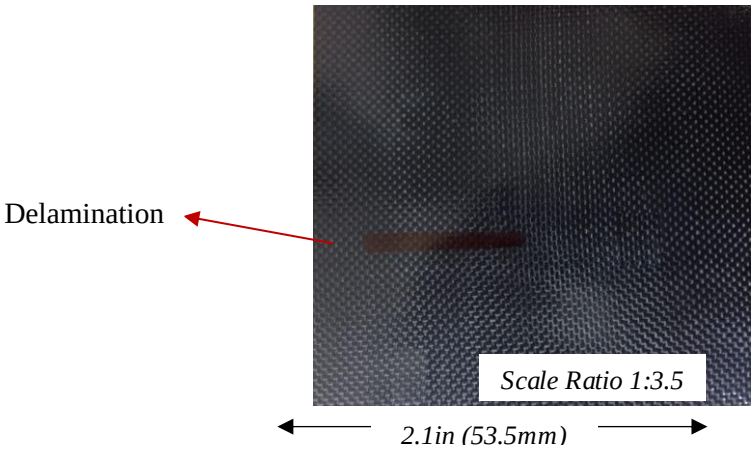


**Fig. 2.** Laminated carbon composite with delamination damage.

**Table 1.** Material properties of the specimen [30]

| Material | $E_{11}$(Gpa) | $E_{22}$(Gpa) | $E_{33}$(Gpa) | $\upsilon_{12}$ | $\upsilon_{13}$ | $\upsilon_{23}$ | $G_{12}$(Gpa) | $G_{13}$(Gpa) | $G_{23}$ (Gpa) | $\rho(kg/m^3)$ |
|---|---|---|---|---|---|---|---|---|---|---|
| | 55 | 55 | 8.265 | 0.06 | 0.437 | 0.437 | 4.0 | 2.407 | 2.407 | **1605** |

**Table 2.** Properties of piezoelectric sensor [30]

| *Piezoceramic* | *tgδ* | *d33 (PC/N)* | *E* | $f_r$ *(hz)* | $f_a$ *(hz)* | $K_p$ *(%)* |
|---|---|---|---|---|---|---|
| $(Ba_{0.95}Ca_{0.05})(Ti_{0.91}Sn_{0.09})O_3$ | 0.027 | 752 | 8100 | 151200 | 179990 | **54.2** |

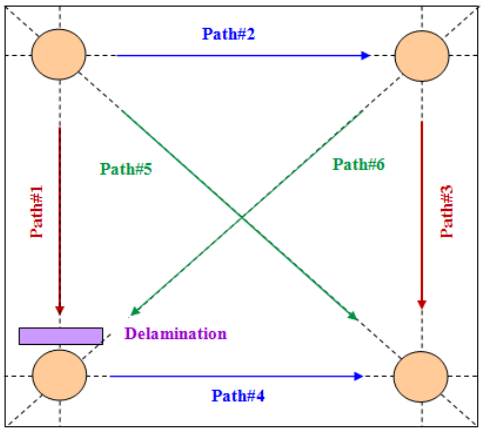


**Fig. 3.** Model description of delamination with the proposed actuator–sensor arrangement

## 2.2. Experimental and numerical setup - Model description

The transducers' wave propagation sensing paths and their deployment scheme on the structure are the same as the test model (Fig. 3). The function generator (RIGOL DG1022) generated a 250kHz and 4cycle burst-sine ultrasonic signal with a 10-V peak-to-peak amplitude and was applied to the BCTS actuators for exciting the structure. A digital oscilloscope collected signals from the sensing Paths 1 to 6 sensors. Fig. 4 shows the experimental setup. In this research, the lamb waves propagation in a square carbon/epoxy was laminated composite plate simulated numerically using the full 3D FEM models and dynamic explicit time-step analyzing ability of the ABAQUS software. The explicit solver can make a better trade-off between computational time and accuracy. In the dynamic time-step analysis, the accuracy and stability of the numerical solution are highly dependant on the spatial and temporal resolution of the analysis. In many investigations, a minimum of twenty points/wave cycles at the highest frequency is set for a time-step resolution. The size of the element is limited to 10% of the wavelength propagated in the structure for obtaining spatial accuracy. Three elements are considered through the thickness of each layer of the plate. The BCTS actuators and composite plate were simulated using an 8-node standard solid element C3D8R with 3 degrees of freedom/node from the ABAQUS element library. The layers were attached by defining the 'tie' constraint between the nodes at the interface of two adjacent layers. Two lower surfaces of BCTS actuators were also attached to the upper surface of the composite plate by 'tie' constraint in ABAQUS/explicit.

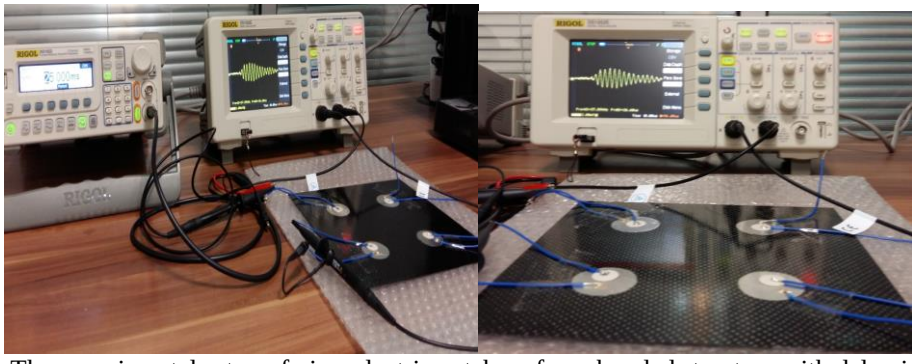

**Fig. 4**. The experimental setup of piezoelectric patch surfaces bonded structure with delamination.

Several works using conventional FEM have simulated the propagation of Lamb waves in structural components [29,31-37]. The studies have shown that a good discretization through the sample thickness (> 3 or 4 layers of elements) is needed to obtain precise results from simulating the $A_0$ mode. The explicit solver makes better trade-offs between computational time and accuracy. To accurately simulate the wave propagation, the model was meshed by 8-node 3D brick with 12 elements, with 4 element layers through the plate thickness (3 elements for each layer). At least 10 main nodes were assigned at the Lamb wavelength to show the validity of each simulated dynamic response. A surface contact algorithm [15] was introduced for processing the contact problem caused by delamination. By an element-based deformable surface, both the lower and upper delamination surfaces were defined. This surface allows the 2 surfaces to interact in a normal direction but resisting mutual penetration. The specifications of the simulated transducers, which were designed and built by the same authors, can be found in their most recent article.

Considering the piezo element's elastic effect, the piezoelectric sensor modeling attached to the structure leads to a more realistic simulation. The lower BCTS surface was attached to the composite plate by the tie constraint in ABAQUS. In addition, 2 connected regions were set as equal. In the tie constraint, the sensor surface and the actuator transducer surface were considered as the slave and master regions, respectively. The recorded signals from all sensing paths were compared between the experiment and the FEM simulation. For example, in Fig. 5, sensing path#3 is compared between the FEM and the experiment. As shown in Fig. 5, a great agreement can be seen for the $S_0$ mode used in detecting damages. Slight differences in amplitude and phase may be due to the adhesive bonding. $S_0$ mode at a relatively high frequency was used for the detection of the delamination damage. As seen in Fig. 5, the antisymmetric part of the signal recorded in the experiment is different from that of the FEM simulation. Therefore, this simulation could only help to design the structural health monitoring asset when only the first symmetric mode of the received signal is used for damage identification.

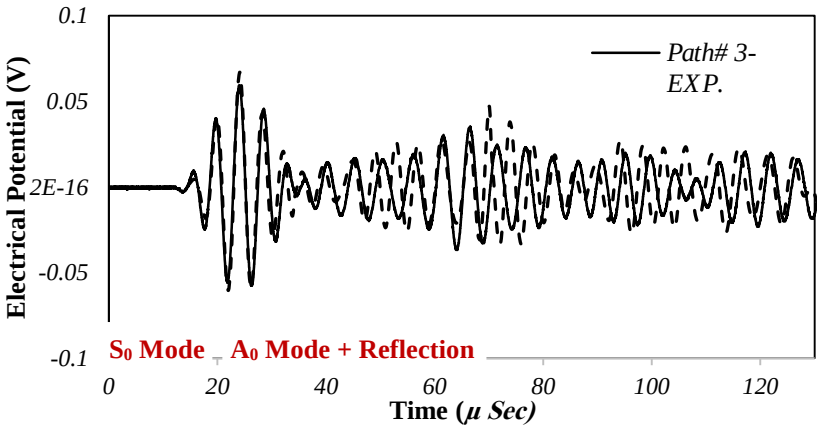


**Fig. 5.** Comparison of the recorded signals from sensing path#3 between the experiment and FEM at fc=250 kHz

### 2.3. Frequency selection

The excitation signal frequency should be correctly chosen to detect damages more precisely. The frequency selection range is completely liberal when one deals with the damages characterized by contact nonlinearity such as delamination. The number and frequency of the signals' cycles were calculated based on the output antisymmetric and symmetric signals. This calculation is dependant on the distance between the sensor and actuator transducers and the velocity of antisymmetric and symmetric waves or waves' time flight. The reason is that the contact nonlinearity arises due to relatively large stiffness alterations at the contact interfaces. The authors did five experiments at different frequencies (50-300 kHz) that the fewer Lamb wave modes are excited in the structure. Besides, a 4-cycle Hanning sinusoidal burst excitation wave with 10V amplitude and 250kHz central frequency was selected for the actuator signal.

### 2.4. Evaluating delamination procedure

The instantaneous baseline damage detection technique requires no pre-recorded data from the pristine structure [38]. It is because the signals recorded from 2 similar or equal paths are the same in the absence of defects near sensing paths. The damage parameters e.g., size, depth, and location of the defect, were extracted by determining the differences between the signals recorded along 2 equal sensing paths with/without damages. In general, signal measurement features response, including phase shift and attenuation, can be utilized to extract damage data of the inspected system due to discontinuities [6]. The output signal feature of similar sensing paths is identical about a simple structure, in the pristine state or health condition.

However, due to the waves reflected from structure edges and material orientation properties in composite and complex structures, their sensing signals are not the same even if equal lengths are considered for all similar sensing paths. Therefore, this study examined the semi-instantaneous baseline damage detection method for damage identification in composite structures [30]. An IC was defined for each of the paths. The "ICi" of the ith sensing path in the pristine conditions is the ratio of the minimum or maximum value of the signal feature content in all paths to the value of the signal energy content in the desired path. The selection of maximum and minimum will be explained in the following. Continuous wavelet transform CWT is a popular signal processing tool to identify the various features of dispersive guided wave signals [9,32,39-41]. The CWT of a guided wave signal is a transformation, which decomposes every such wave into a superposition of both translation and scale of a mother wavelet function $\psi(t)$ given by

$$\psi_{a,\tau}(t) = |a|^{\frac{-1}{2}}\psi\left(\frac{t-\tau}{a}\right) \quad (1)$$

In the above-mentioned equation, the scaling parameter "a" controls the wavelet frequency bandwidth, and the translation parameter "$\tau$" shifts the wavelet in time. The CWT of a time-domain guided wave signal "S(t)" is defined as follows:

$$W_{\psi}(a,\tau) = \frac{1}{\sqrt{a}}\int_{-\infty}^{\infty} s(t)\,\psi^{*}\left(\frac{t-\tau}{a}\right) d(t) \quad (2)$$

where $\psi^*$ is the complex conjugate of $\psi$. The wavelet energy spectrum "Ei(t, f)" for the ith path is:

$$E_i(t,f) = |W_i(t,f)|^2 \quad (3)$$

"Wi(t,f)" is the scalogram related to the ith sensing path. Therefore, the value of feature content (the energy index of each path or the wavelet energy value) related to the ith sensing path "Fi" is defined as

$$F_i = \int_{t_i}^{t_e} E_i\,(t,f^{*})dt \quad (4)$$

In equation 4, $t_e$ and $t_i$ are the end and initial times of the windowed segment of the signal received, and f* is the frequency or scale where the absolute value of the CWT coefficients $|Wi(t, f)|$ is maximized [29].

The semi-instantaneous method used here is based on the fact that each sensing feature must be normalized to the healthiest sensing path by the identical coefficient calculated in pristine conditions. For delamination defects, the feature content value of the output signal recorded from a path with delamination through that is higher than from the same path with no damage. This phenomenon will be shown in the result section by comparing the output waveform, output signal recorded from a path in health and damaged condition. This is because, in a composite structure such as a composite plate, the transducers are attached to the upper layer. When a Lamb wave is excited in the structure by the actuator transducer, the wave propagated in the structure through the laminate, attaching the transducer and other lower laminates by transferring the wave energy through the interference between the layers. Therefore, when there is a delamination defect between the layers, lower wave energy transfers to the lower layers. S0, the wave energy content value recorded from sensing the damaged path, contains a delamination defect trough that is higher than that of without delamination. However, the defects such as fatigue cracks cause a discontinuity in structure, and the wave amplitude is decreased when it passes through the fatigue cracks like to the cut trough damages. Therefore, an IC is defined for each path. The IC of each sensing path is equal to the ratio of the highest amount of the signal energy of all paths to the amount of signal energy of the desired path [29] to identify the fatigue cracks in metallic lap-joint structures. In this research, because of the identification of the delamination defects, the "$IC_i$" of the ith sensing path is as follows:

$$IC_i = \frac{F_{Min}^{P}}{F_i^{P}} \quad (5)$$

where "$F_i^P$" is the value of the wavelet energy content of the ith sensing path in pristine condition and "$F_{Min}^P$" is the minimum value of the wavelet energy content of the signals present in all the existing sensing paths. Then, by multiplying the value of the current energy content "$F_i^C$" of the ith sensing path "$F_i^C$" and its "$IC_i$" , the value of adjusted energy feature "$F_i^{ad}$" of the sensing path at the current measurement condition is obtained by $F_i^{ad}$

$$F_i^{ad} = IC_i \times F_i^{C} \quad (6)$$

This *IC* eliminates the effect of differences in path length and other factors that affect path energy. When there is no damage to the sensing paths, the values of adjusted energy in all sensing paths are identical at any current measurement data. The "$DI_i$" of the ith sensing path is as follows:

$$DI_i = \left|\frac{F_{Min}^{ad} - F_i^{ad}}{F_{Min}^{ad}}\right| \quad (7)$$

where "$F_{Min}^{ad}$" is the minimum value in the adjusted energy of all sensing paths.

There is no need to refer to the collected pristine data in future detection procedures due to the difference between this method and baseline methods. $S_0$, operational and environmental conditions can not affect the results of damage detection. In addition, IC is used to remove errors due to some uncertainties like plate thickness alterations, dimension inaccuracy during assembly and manufacturing procedures, embedded sensor dislocation, orientation layer, and laying up the process in the damage detection results. Even when the structure is in good condition, these

inaccuracies or uncertainties lead to differences in the sensing signals of similar paths. Thus, if IC is not used, the instantaneous baseline damage index may falsely show some damage in undamaged structures, or one may have to set high threshold values for the indices. In this algorithm, it is assumed that there is more than one healthy sensing path among all similar or equal sensing paths for the designed actuator-sensor arrangement. So, it can detect various damaged paths.

## 3. Results and discussion

### 3.1. Delamination detection by comparing the output signal of the sensing paths

In this study, the method for identifying semi-instantaneous baseline damage was developed and modified. Experimental tests were conducted to investigate the recorded signal and delamination damage detection. A 250kHz frequency excitation wave was chosen as an exciting wave in the composite plate structure because it provides good separation between the "$A_0$" and "$S_0$" modes in all sensing paths. The received signal represents the baseline signal, and shows the response time signal when delamination is within a direct line of the actuator and sensor path. The response signal is composed of several wave modes owing to wave scattering at the boundaries. In Fig. 5, the first mode, which looks like a sine wave modulated by a cosine function, is the first arrival of the $A_0$ mode associated with the direct path of the wave propagation. The second mode is another $A_0$ mode that is reflected from the edge of the plate. The observation of Fig. 5 clearly reveals that the first $A_0$ mode is the most sensitive to delamination damage. Based on these observations, a damage index is defined as the function of a signal's attenuation at a limited time span (a signal portion corresponding to the first $A_0$ mode) and at a specific frequency (the input frequency of the signal). Considering the necessary conditions that enforce the application of "IC" to the DI of similar sensing paths (i.e., symmetry in placing, geometry, and materials), the collected data for path#2 should be identical to the signals obtained from path#4. In fact, paths 2 and 4 are mirror symmetries of each other, without any damage .The corresponding wave packet consists of the first symmetric mode ($S_0$), the first antisymmetric mode ($A_0$), and the reflected wave from the boundaries. The ICs for all sensing paths (i.e., paths 1 to 6 as described in Fig. 3) are obtained. $S_0$ mode at relatively high frequency was used for the detection of the delamination damage.

Fig. 6 a and b compares the recorded signal of the sensing path#1 and #3, respectively, for two samples (one without any damage and the other having a peeling defect in thought path#1 as shown in Fig. 1). Results of Fig. 6a illustrate that the amplitude of the output recorded signal will be increased due to the existence of delamination defects in sensing path#1. Also, there is no difference in the amplitude of the output recorded signal in sensing path#3 for two samples.

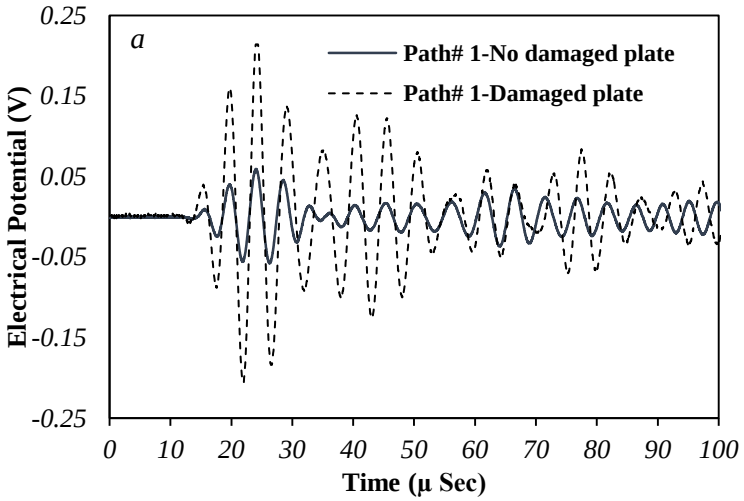

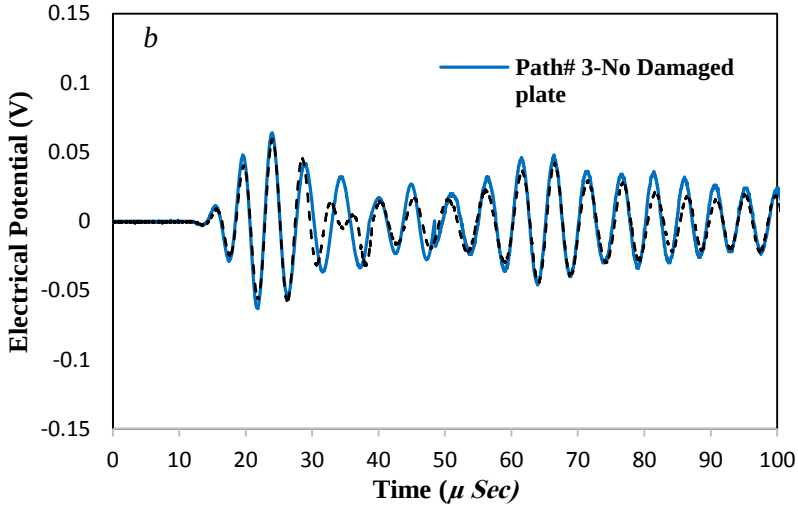


**Fig. 6.** Comparing the recorded signal of (a) sensing path #1, and (b) sensing path #3 for two un-damaged and damaged composite plate samples.

### 3.2. Sensing paths ICs

The ICs can eliminate the effect of uncertainty that occurred during production and measurement processes such as geometry, variable thickness, layer arrangement, plies angle, manufacturing, and installation condition. The IC is obtained for all sensing paths in the pristine condition of undamaged samples and reflects the relationship between the signals of the structure used to eliminate any present inequalities in each path. The proposed ICs modify the DI values for all sensing paths to remove the errors due to reflections from structural components and boundaries. ICs are only needed to be calculated once at the design stage of the SHM system. These coefficients that reflect the relationship between the paths are different from the recorded baseline data and are obtained when the structure is in its pristine condition. The ICs for all sensing paths in the pristine condition of the structure is obtained and utilized to eliminate the inequalities that occurred in the signals of each path. In this study, for delamination damage detection in the laminated composite plate, there are three groups of equal sensing paths: group paths 1 (paths#1 and #3), group paths 2 (paths#2 and #4), and group paths 3 (paths#5 and #6). Fig. 7 shows the ICs of all six sensing paths, calculated by the experimental output results of two samples. The standard deviation of ICs difference between paths #1 and #3 in group paths 1, path#2, and #4 in group paths 2, and path#5 and #6 in group paths 3, are 0.004, 0.005, and 0.005, respectively. These differences refer to measurement, equipment, manufacturing errors, etc. The ICs differences between group paths 1, group paths 2, and group paths 3, are due to differences in the length of the measurement paths.

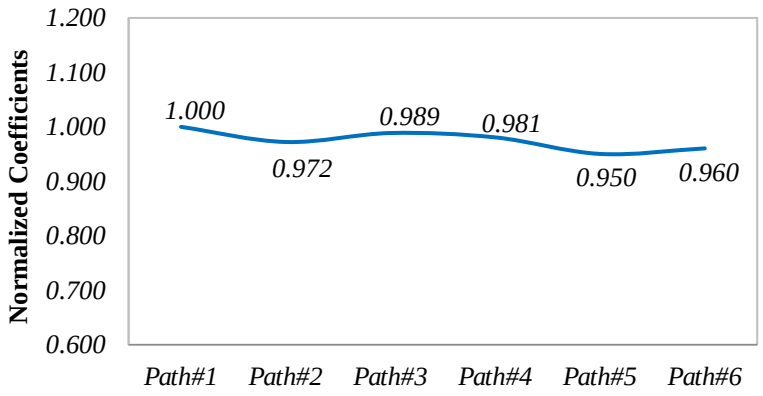


**Fig. 7.** IC values of Sensing Paths 1 to 6.

### 3.3. DI values

Fig. 8 shows the DI for six sensing paths. The path with damage (path#1) is identified by its higher index value. Higher threshold values are required because of the presence of some noise signals from the environmental impacts and measuring tools. Here a threshold value of 0.04 is sufficient. So, the values of the index produced by damages were significant against the threshold value set. The errors were less than 4%, which may be related to the linear relationship considered for the DI and delamination damage (Fig. 8). Recognition of the damaged path is difficult, with very low values of DI [29]. However, baseline-free methods play a significant role in removing such drawbacks as noise signals from the manufacturing process, measuring tools, etc. Therefore, with the proposed damage technique, several damaged paths can also be detected if there is a path without any damage. The output wave signals for damaged and undamaged samples (with delamination damage in path#1) were investigated by the experiment. Comparison of the results of recorded signals from sensing path for two healthy and damaged samples using two experimental and FEM analysis methods shows a significant difference between two samples in path#1 (the path with delamination damage). Also, it was not observed any notable difference in path#3 between undamaged and damaged samples. So, the damage was identified, and the performance of the lead-free piezoelectric sensors was verified. The delaminated damage was detected because the delamination phenomenon increased the amplitude of the wave and the wave energy.

A comparison of the DI values for six sensing paths based on the semi instantaneous baseline method shows that path#1 has the highest DI=0.92. In addition, DI of path#4 due to closeness to delamination damage is DI=0.67. Path#6 with a distance farther from the damage shows DI=0.09. Other sensing paths i.e. path#2, #3 and #5 with DI are close to zero due to no damage (Fig. 8).

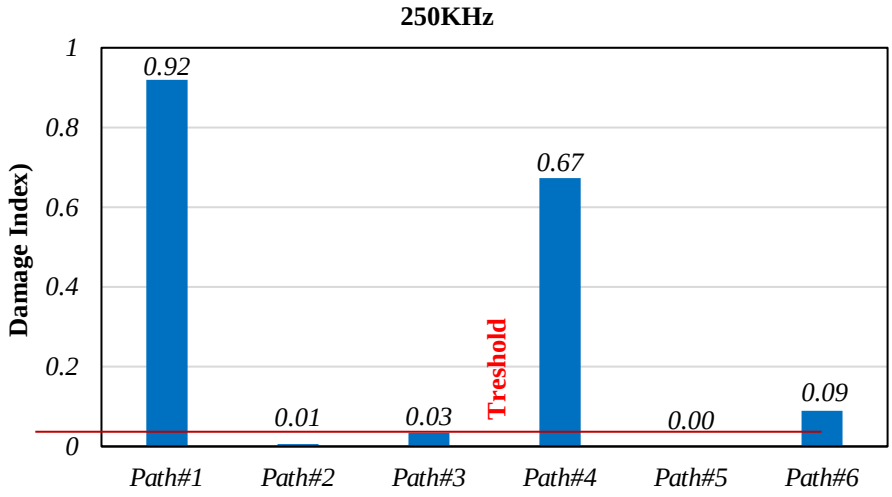


**Fig. 8.** DI values of Sensing Paths#1 to #6

## 4. Conclusions

In this paper, a semi-instantaneous baseline algorithm based on the wave propagation technique was developed in a carbon composite plate containing delamination damage by using an active sensing network with four (BCTS) lead-free piezoelectric transducers. The electrical signals' excitation forces applied to the piezoelectric actuators were calculated and entered into the model. The Lamb wave was created by imposing force profiles with time change to the actuator transducer nodes. The IC is obtained for all sensing paths in the pristine condition of undamaged samples and reflects the relationship between the signals of the structure used to eliminate any present inequalities in each path. The proposed ICs modify the DI values for all sensing paths to remove errors due to structural components and boundaries reflections. This can also reduce the uncertainty caused in manufacturing and assembly processes, that is, geometrical asymmetries and length differences in sensing paths. ICs are only needed to be calculated once at the design stage of the SHM system. These coefficients that reflect the relationship between the paths are different from the recorded baseline data and are obtained when the structure is in its pristine condition. The values of the index produced by damages were significant against the threshold value set. The errors were less than 4%, which may be related to the linear relationship considered for the DI and delamination damage. The output wave signals of samples were investigated by experiment and FEM (using Abaqus software). A comparison of the results of recorded signals from sensing paths shows a significant difference between the two healthy and damaged samples. The delaminated damage was detected because the

delamination phenomenon increased the amplitude of the wave and the wave energy. $S_0$ mode at a relatively high frequency was used for the detection of the delamination damage. A comparison of the DI values of six sensing paths shows that the path with delamination damage (path#1) has the highest DI value i.e., 0.92 and then the sensing paths closest to the damage show the highest DI values. The DI values of other sensing paths are close to zero due to no damage. So, the damage was identified, and the performance of the BCTS sensors was verified.

## Data Availability

All data, models, and code generated or used during the study appear in the submitted article.

## References

[1] D. Alleyne, P. Cawley, "A two-dimensional Fourier transform method for the measurement of propagating multi mode signals", Acoust. Soc. Am. J., Vol. 89, 1991, pp. 1159-1168.

[2] Clarke TF. Simonetti, P. Cawley, "Guided wave health monitoring of complex structures by sparse array systems: Influence of temperature changes on performance", Sound Vib. J., Vol. 329, 2010, pp. 2306-2322.

[3] ] K. Diamanti, J. Hodgkinson, C. Soutis, "Detection of Low-velocity Impact Damage in Composite Plates using Lamb Waves", Struct. Health Monit. J., Vol. 3, 2004, pp. 33-41.

[4] V. Giurgiutiu, "Tuned Lamb Wave Excitation and Detection with Piezoelectric Wafer Active Sensors for Structural Health Monitoring", Intell. Mater. Syst. Struct. J., Vol. 16, 2005, pp. 291-305.

[5] H. W. Park, H. Sohn, "Time reversal active sensing for health monitoring of a composite plate", Sound Vib. J., Vol. 302, 2007, pp. 50-66.

[6] A. Raghavan, C. E. Cesnik, "Review of Guided-Wave Structural Health Monitoring", Shock Vibr. J., Vol. 39, 2007, pp. 91-114.

[7] P. Rizzo, E. Sorrivi, F. Lanza di Scalea, E. Viola, "Wavelet-based outlier analysis for guided wave structural monitoring: Application to multi-wire strands", Sound Vib. J., Vol. 307, 2007, pp. 52-68.

[8] Z. Su, X. Wang, Z. Chen, L. Ye, D. Wang, "A built-in active sensor network for health monitoring of composite structures", Smart Mater. Struct. J., Vol. 15, 2006, pp. 1939-1947.

[9] G. Yan, "A Bayesian approach for damage localization in plate-like structures using Lamb waves", Smart Mater. Struct. J., Vol. 22, 2013, pp. 12-35.

[10] H. Sohn, H. W. Park, K. H. Law, C. R. Farrar, "Combination of a Time Reversal Process and a Consecutiv Outlier Analysis for Baseline-free Damage Diagnosis", Intell. Mater. Syst. Struct. J., Vol. 18, 2007, pp. 335-346.

[11] ] D. W. Greve, J. J. Neumann, J. H. Nieuwenhuis, I. J. Oppenheim, N. L. Tyson, "Use of Lamb waves to monitor plates: experiments and simulations", Proc. SPIE, Vol. 5765, Smart Struct. and Mater. , Sensors and Smart Struct., Technologies for Civil, Mechanical, and Aerospace Systems, Vol. 3, 2005, pp. 117-129.

[12] M. Lowe, O. Diligent, "Low-frequency reflection characteristics of the $S_0$ Lamb wave from a rectangular notch in a plate", Acoust. Soc. Am. J., Vol. 111, 2002, pp. 64-76.

[13] J. Rajagopalan, K. Balasubramaniam, C. Krishnamurthy, "A single transmitter multi receiver (STMR) PZT array for guided ultrasonic wave based structural health monitoring of large isotropic plate structures", Smart Mater. Struct. J., Vol. 15, 2006, pp. 1190-1198.

[14] P. Malinowski, T. Wandowski, I. Trendafilova, W. Ostachowicz, "Optimization of sensor placement for structural health monitoring: a review", Struct. Health Monitor. J., Vol. 18, 2019, pp. 963-988.

[15] B. Alem, A. Abedian, K. Nasrollahi-Nasab, "Reference-Free Damage Identification in Plate-Like Structures Using Lamb-Wave Propagation with Embedded Piezoelectric Sensors", Aerosp. Eng. J., Vol. 29, 2016, pp. 04016062-1 - 04016062-13.

[16] C. Q. Gómez Muñoz, F. P. García Marquez, B. H. Crespo, K. Makaya, "Structural health monitoring for delamination detection and location in wind turbine blades employing guided waves", Wind Energy J. , Vol. 22, 2019, pp. 698-711.

[17] M. Gresil V. Giurgiutiu, "Guided wave propagation in carbon composite laminate using piezoelectric wafer active sensors", Smart Mater. Struct. J., Vol. 16, 2013, pp. 75-88.

[18] C. M. Yeum, H. Sohn, J. B. Ihn, H. J. Lim, "Instantaneous delamination detection in a composite plate using a dual piezoelectric transducer network", Compos. Struct. J., Vol. 94, 2012, pp. 3490-3499.

[19] V. Giurgiutiu and G. Santoni-Bottai, "Structural health monitoring of composite structures with piezoelectric wafer active sensors", AIAA J., Vol.49, 2011, pp. 565-581.

[20] H. W. Park, H. Sohn, K. H. Law, C. R. Farrar, "Time reversal active sensing for health monitoring of a composite plate", Sound Vib. J., Vol. 302, 2007, pp. 50-66.

[21] H. Sohn, H. W. Park, K. H. Law, C. R. Farrar, "Damage detection in composite plates by using an enhanced time-reversal method", Aerosp. Eng. J., Vol. 20, 2007, pp. 141-154.

[22] K. Kyoung-Tak, C. Heoung-Jae, S. Joo-Hyun, L. Jin-Ah, B. Joon-Hyung, U. Moon-Kwang, L. Sang-Kwan, J. Ju-Woong, "Quantitative

Accessibility of Delamination in Composite Using Lamb Wave by Experiments and FEA", Adv. Compos. Mater. J., Vol. 20, 2011, pp. 361-373.
[23] CT Ng, H. Mohseni, HF Lam, "Debonding detection in CFRP-retrofitted reinforced concrete structures using nonlinear Rayleigh wave", Mech. Syst. Sig. Proc. J., pp. 245-256.
[24] H. Sohn, "Effects of environmental and operational variability on structural healthmonitoring" , Philosophical Trans. R. Soc. A: Proc. Math., Phys. Eng. Sci. J., Vol. 365, 2007, pp. 539-560.
[25] A. Marzani, S. Salamone, "Numerical prediction and experimental verification of temperature effect on plate waves generated and received by piezoceramic sensors", Mech. Syst. Sig. Proc. J., Vol. 30, 2012, pp. 204-217.
[26] S. Roy, K. Lonkar, V. Janapati, F. K. Chang, "A novel physics-based temperature compensation model for structural health monitoring using ultrasonic guided waves", Struct. Health Monitor. J., Vol. 13, 2014, pp. 321-342.
[27] G. B. Santoni, L. Yu, B. Xu, V. Giurgiutiu, "Lamb Wave-Mode Tuning of Piezoelectric Wafer Active Sensors for Structural Health Monitoring", Vib. Acoust. Trans. ASME J., Vol. 129, 2007, pp. 752-762.
[28] S. B. Kim, H. Sohn, "Instantaneous reference-free crack detection based on polarization characteristics of piezoelectric materials", Smart Mater. Struct. J., Vol. 16, 2007, pp. 2375-2384.
[29] B. Alem, A. Abedian, "A semi-baseline damage identification approach for complex structures using energy ratio correction technique", Struct. Cont. Health Monitor. J., Vol. 25, 2018.
[30] M.H. Ataei, S.A Hassanzadeh-Tabrizi, M.Rafiei, A. Monshi, "Design development of $(Ba_{1-x}Ca_x)(Ti_{1-y}Sn_y)O_3$ lead-free piezo ceramic by two manufacturing methods of CSS and SPS, promising for delamination damage detection", Alloys Compd. J., Vol. 795, 2019, pp. 197-206.
[31] H. Cho, C. J. Lissenden, "Structural health monitoring of fatigue crack growth in plate structures with ultrasonic guided waves", Struct. Health Monitor. J., Vol. 11, 2012, pp. 393-404.
[32] A. Bagheri, K. Li, P. Rizzo, "Reference-free damage detection by means of wavelet transform and empirical mode decomposition applied to Lamb waves", Intell. Mater. Syst. Struct. J., Vol. 24, 2013, pp. 194-208.
[33] F. Moser, L. J. Jacobs, "Modeling elastic wave propagation in waveguides with the finite element method", NDT Int. J., Vol. 32, 1999, pp. 225-234.
[34] I. Bartoli, F. L. di Scalea, M. Fateh, E. Viola, "Modeling guided wave propagation with application to the long-range defect detection in railroad tracks", NDT Int. J., Vol. 38, 2005, pp. 325-334.
[35] L. De Marchi, A. Marzani, N. Speciale, E. Viola, "A dispersion compensation procedure to extend pulse-echo defects location to irregular waveguides", NDT Int. J., Vol. 54, 2013, pp. 115-122.
[36] M. Sale, P. Rizzo, A. Marzani, "Semi-analytical formulation for the guided waves-based reconstruction of elastic moduli", Mech. Syst. Sign. Process J., Vol. 25, 2011, pp. 2241-2256.
[37] H. W. Park, S. B. Kim, H. Sohn, "Understanding a time-reversal process in Lamb wave propagation", Wave Motion J., Vol. 46, 2009, pp. 451-467.
[38] S. R. Anton, D. J. Inman, G. Park, "Reference-free damage detection using instantaneous baseline measurements", AIAA J., Vol. 47, 2009, pp. 1952-1964.
[39] H. Sohn, G. Park, J. R. Wait, N. P. Limback, C. R. Farrar, "Wavelet-based active sensing for delamination detection in composite structures", Smart Mater. Struct. J., Vol. 13, 2004, pp. 153-164.
[40] S. A. Atashipour, H. R. Mirdamadi, M. H. Hemasian-Etefagh, "An effective damage identification approach in thick steel beams based on guided ultrasonic waves for structural health monitoring applications", Intell. Mater. Syst. Struct. J., Vol. 24, 2013, pp. 584-597.
[41] X. Zhao, H. Gao, G. Zhang, B. Ayhan, F. Yan, C. Kwan, J. L. Rose, "Active health monitoring of an aircraft wing with embedded piezoelectric sensor/actuator network: I. Defect detection, localization and growth monitoring", Smart Mater. Struct. J., Vol. 16, 2007, pp. 1208-1219.